ASSESSMENT OF THE TURBULENCE MODELS FOR MODELLING OF BUBBLE COLUMN

(Date received: 1.7.2009)

Jolius Gimbun
Faculty of Chemical and Natural Resources Engineering,
Universiti Malaysia Pahang, Lebuhraya Tun Razak,
26300 Gambang, Pahang
E-mail: j.gimbun@gmail.com

ABSTRACT

This paper presents an Eulerian two-fluid modelling of the gas-liquid flow in a bubble column. The influence of the bubble size, turbulence models and the grid size on the gas hold-up and the axial liquid velocity were evaluated. The results for the gas hold-up and liquid axial velocity shows good agreement with experimental data from literature. The modelling results suggest that the two-phase k-ε turbulence model is more appropriate for bubble column operating at high gas loading (of approx. 30% hold-up) and the assumption of a monodispersed bubble size is adequate for bubble column simulation.

Keywords: *Bubble Column, Computational Fluid Dynamics, Gas-liquid, Multiphase Modelling, and Turbulence Model*

1.0 INTRODUCTION

A bubble column is a simple unit in which a continuous gas phase in form of bubble moves relative to the continuous liquid phase. Bubble columns usually used as reactors in variety of chemical and biochemical processes, such as oxidation reactions (*e.g.* [1-2]), cell cultures (*e.g.* [3]), alkylation reactions (*e.g.* [4]), effluent treatment (*e.g.* [5]), Fischer-Tropsch synthesis (*e.g.* [6]) and coal liquefaction (*e.g.* [7]). Bubble columns had an advantage of being mechanically simple without present of any internal structure or moving part, thus leading to easier maintenance. They also have high mass transfer rates between the gas and liquid phases, good heat transfer characteristics and large liquid hold-up, which are favourable to slow liquid phase reactions [8]. Operation of bubble columns is often determined by several global parameters such as pressure drop, aeration height and gas superficial velocity. However, the variables that affect the performance of bubble column are the gas hold-up distribution, gas-liquid mass and heat transfer coefficients, the extent of mixing, bubble rise velocities and bubble size distributions. It is possible to measure these variables experimentally using, for example, a combination of several instruments such as the laser doppler anemometry, dissolved oxygen probe, X-ray tomography and digital imaging. However, experimental measurements require investing in costly instruments and building a prototype. Alternatively, these parameters can also be obtained from CFD simulations, which offer a cheaper but much faster solution.

There are many published works related to bubble column modelling ranging from a simple 1D [9] to a 3D model [10-11] and some even incorporated the bubble size distributions *i.e.* population balance model [12-14]. Usually the Eulerian two-fluid model is employed to solve the two-phase problem and the dispersed *k*-ε model is used for turbulence modelling. More elaborated turbulence model such as the large eddy simulation (LES) had also been employed recently to model the two-phase flow in the bubble column [10,15]. According to Dhotre *et al*. [15], predictions of the mean flow field (mean velocities, mean gas hold-up) and turbulent kinetic energy obtained using the *k*-ε models are comparable to those obtained using LES for the case of a bubble column. This is due to the fact that there are little chances of a high gradient flow (due to jet) or a wake flow (due to internal structure or impeller rotation) to develop in a bubble column due to its simple structure. Of course the LES is a better turbulence model than the *k*-ε model for predicting the turbulent flow feature such as the velocity fluctuations. However, LES requires much higher computational effort due to needs of finer grid to better resolve the eddy structure. Since the *k*-ε model is capable of predicting the mean flow field satisfactorily in the bubble column, thus the *k*-ε model was chosen instead of LES for the purpose of this study.

The previous study also often deals with air-water system with air superficial velocity ranging from 0.012 to 0.12 m/s. There are two types of the commonly studied bubble column *i.e.* rectangular and cylindrical shape. Most of the studies [9-11, 15-17] employed a constant bubble size in their model either taken from experimental observation, or computed using published correlations. Both the lift and virtual mass forces are often omitted from the simulation but the drag coefficient is applied. Interestingly, most of the CFD studies on bubble columns were able to predict correctly the gas hold-up and liquid axial velocity even without applying the bubble size distribution model. The reason is that there is little chance of forming a bubble breakage dominated system in a bubble column and most of the coalescence taking place near the sparger. Bubble breakage occurs due to high

gradient of turbulent kinetic energy and dissipation rates, which is often induced by mechanical moving part *i.e*. impeller. In the case of bubble column, the flow is only driven by the bubble rise motion and the resultant turbulent flow is not sufficient to imply a bubble breakage dominated system. That leaves the bubble size almost constant throughout the column thus eliminating the vital needs of the population balance model (PBM). Chen *et al*. [12] employed a PBM in their work, and they compared the result with the one without PBM. Their modelling was carried out in a 2D domain. According to Chen *et al*. [12], CFD simulation using a monodispersed bubble size itself can match the result from a more complicated CFD-PBM. This is due to the fact that bubble size in a bubble column is virtually monodispersed and hence can be represented by the mean bubble size during the CFD simulation. Similar observation was also reported by Groen [18] who performed detailed experimental measurement on bubble size distribution in a bubble column.

Despite many published work on CFD of bubble columns, selection of turbulence models is still not clearly understood. To the author's knowledge, such a study has not yet been undertaken and that is the aim of this work. In this work, three different turbulence models namely mixture *k*-ε, dispersed *k*-ε and two-phase *k*-ε were employed to predict the hydrodynamics of a bubble column operating at a relatively high superficial gas velocity of 0.12 m/s, which corresponds to 30% gas hold-up.

2.0 MODELLING APPROACH

2.1 CFD modelling of two-phase flow

The Eulerian-Eulerian approach is employed for gas-liquid bubble column simulation in this work, whereby the continuous and disperse phases are considered as interpenetrating media, identified by their local volume fractions. The volume fractions sum to unity and are governed by the following continuity equations:

$$\frac{\partial}{\partial t}(\alpha_l \rho_l) + \nabla \cdot (\alpha_l \rho_l \vec{u}_l) = 0 \tag{1}$$

where α_l is the liquid volume fraction, ρ_l is the density, and $\vec{u}_l$ is the velocity of the liquid phase. The mass transferred between phases is negligibly small and hence is not included in the right hand-side of *eq*.(1). A similar equation is solved for the volume fraction of the gas phase by replacing the subscript *l* with *g* for gas. The momentum balance for the liquid phase is:

$$\frac{\partial}{\partial t}(\alpha_l \rho_l \vec{u}_l) + \nabla \cdot (\alpha_l \rho_l \vec{u}_l \vec{u}_l) = -\alpha_l \nabla P + \nabla \cdot \bar{\bar{\tau}}_l + \vec{F}_{lg} + \alpha_l \rho_l \vec{g} + \vec{F}_{lift,l} + \vec{F}_{vm,l} \tag{2}$$

where $\bar{\bar{\tau}}_l$ is the liquid phase stress-strain tensor, $\vec{F}_{lift,l}$ is a lift force, $\vec{g}$ is the acceleration due to gravity and $\vec{F}_{vm,l}$ is the virtual mass force. A similar equation is solved for the gas phase. $\vec{F}_{lg}$ is the interaction force between phases, due to drag. Hence, $\vec{F}_{lg}$ is represented by a simple interaction term for the drag force, given by:

$$\vec{F}_{lg} = -\frac{3\alpha_g \alpha_l C_D |\vec{u}_g - \vec{u}_l| (\vec{u}_g - \vec{u}_l)}{4 d_b} \tag{3}$$

where C_D is a drag coefficient and d_b is the Sauter mean bubble diameter.

The drag model employed has a significant effect on the flow field of the aerated flow, as it is related directly to the bubble terminal rise velocity. The drag model given as a function of the bubble Reynolds number, Re_b, from Schiller and Naumann [19] was employed in this work:

$$C_D = \frac{24}{Re_b}(1 + 0.15 Re_b^{0.687}) \tag{4}$$

Lift forces act on a bubble due to the velocity gradients in the liquid phase and are said to be more significant for larger bubbles. The lift force acting on a gas phase in a liquid phase can be estimated from:

$$\vec{F}_{lift,g} = -C_L \rho_l \alpha_g (\vec{u}_l - \vec{u}_g) \times (\nabla \times \vec{u}_l) \tag{5}$$

where C_L is a lift coefficient has a value 0.5. A similar lift force is added to the right-hand side of the momentum equation for both phases ($\vec{F}_{lift,g} = -\vec{F}_{lift,l}$).

The virtual mass effect occurs when a gas phase accelerates relative to the liquid phase. The fluid surrounding the bubble is accelerating as a consequence of the bubble acceleration. This gives a rise to a force called a virtual mass which accounts for the losses of momentum of the accelerating bubble. The virtual mass force acting on bubbles is given by:

$$\vec{F}_{vm,g} = C_m \rho_l \alpha_g \left(\frac{d_l \vec{u}_l}{dt} - \frac{d_g \vec{u}_g}{dt} \right) \tag{6}$$

where C_m is the added mass coefficient has a value 0.5 for sphere. Similar with the lift force the virtual mass force is added to the right-hand side of the momentum equation for both phases ($\vec{F}_{vm,l} = -\vec{F}_{vm,g}$).

2.2 Turbulence modelling

There are three different options available for turbulence modelling of multiphase flow in FLUENT namely the mixture *k*-ε, dispersed *k*-ε and two-phase *k*-ε models [20]. All three turbulence models used the same model constants but has different equations to account for the turbulence viscosity.

Mixture k-ε model

The mixture turbulence model is the default multiphase turbulence model in FLUENT 6.3. It represents the first extension of the single-phase *k*-ε model, and it is applicable when phases separate, for stratified (or nearly stratified) multiphase flows, and when the density ratio between phases is close to 1. In these cases, using mixture properties and mixture velocities is sufficient to capture important features of the turbulent flow.

The *k* and ε equations describing this model are as follows:

$$\frac{\partial}{\partial t}(\rho_m k) + \nabla \cdot (\rho_m \vec{u}_m k_m) = \nabla \cdot \left(\frac{\mu_{t,m}}{\sigma_k} \nabla k \right) + G_{k,m} - \rho_m \varepsilon \tag{7}$$

$$\frac{\partial}{\partial t}(\rho_m \varepsilon) + \nabla \cdot (\rho_m \vec{u}_m \varepsilon) = \nabla \cdot \left(\frac{\mu_{t,m}}{\sigma_\varepsilon} \nabla \varepsilon \right) + \frac{\varepsilon}{k}(C_{1,\varepsilon} G_{k,m} - C_{2,\varepsilon} \rho_m \varepsilon) \tag{8}$$

where the $G_{k,m}$ is the mixture turbulent kinetic production term. The mixture density and velocity, ρ_m and $\vec{u}_m$, are computed from;

$$\rho_m = \sum_{i=1}^{N} \alpha_i \rho_i \tag{9}$$

and

$$\vec{u}_m = \sum_{i=1}^{N} \alpha_i \rho_i \vec{u}_i \Big/ \sum_{i=1}^{N} \alpha_i \rho_i \tag{10}$$

The turbulent viscosity, μ_{tm}, is computed from

$$\mu_{t,m} = \rho_m C_\mu \frac{k^2}{\varepsilon} \tag{11}$$

The model constants are; $C_{\varepsilon 1}$ = 1.44, $C_{\varepsilon 2}$ = 1.2, $C_{\varepsilon 3}$ = 1.2, C_μ = 0.09, σ_k = 1 and σ_ε = 1.3.

Dispersed k-ε model

Dispersed *k*-ε model is suitable when the secondary phase is dilute and the primary phase is clearly continuous, the dispersed *k*-ε turbulence model is used and solves the standard *k*-ε equations for the primary phase. The liquid turbulent viscosity, $\mu_{t,l}$, is written as:

$$\mu_{t,l} = \rho_l C_\mu \frac{k_l^2}{\varepsilon_l} \tag{12}$$

The transport equations for *k* and ε in the dispersed *k*-ε model are given by:

$$\frac{\partial}{\partial t}(\rho_l \alpha_l k_l) + \nabla \cdot (\rho_l \alpha_l \vec{u}_l k_l) = \nabla \cdot \left(\alpha_l \frac{\mu_{t,l}}{\sigma_k} \nabla k_l \right) + \alpha_l G_{k,l} - \alpha_l \rho_l \varepsilon_l + \alpha_l \rho_l \Pi_{k,l} \tag{13}$$

$$\frac{\partial}{\partial t}(\rho_l \alpha_l \varepsilon_l) + \nabla \cdot (\rho_l \alpha_l \vec{u}_l \varepsilon_l) = \nabla \cdot \left(\alpha_l \frac{\mu_{t,l}}{\sigma_\varepsilon} \nabla \varepsilon_l \right) + \alpha_l \frac{\varepsilon_l}{k_l} (C_{1,\varepsilon} G_{k,l} - C_{2,\varepsilon} \rho_l \varepsilon_l) + \alpha_l \rho_l \Pi_{\varepsilon,l} \tag{14}$$

$G_{k,l}$ is the rate of production of turbulent kinetic energy and it has a similar form to the one applied for single phase flow. The terms $\prod_{k,l}$ and $\prod_{\varepsilon,l}$ represent the influence of the dispersed phase on the continuous phase and are modelled following Elgobashi and Abou-Arab [21]. The turbulent quantities for the dispersed phase like turbulent kinetic energy and turbulent viscosity of the gas are modelled following Mudde and Simonin [22] using the primary phase turbulent quantities [20]. The model constants are similar to those of mixture *k*-ε models.

Two-phase k-ε model

The most general turbulence model for multiphase flows solves a set of *k* and ε transport equations for each phase. This turbulence model is the appropriate choice when the turbulence transfer among the phases plays a dominant role *i.e*. high gas void fraction. The transport equations for two-phase *k*-ε model are given by:

$$\frac{\partial}{\partial t}(\rho_l \alpha_l k_l) + \nabla \cdot (\rho_l \alpha_l \vec{u}_l k_l) = \nabla \cdot \left(\alpha_l \frac{\mu_{t,l}}{\sigma_k} \nabla k_l \right) + (\alpha_l G_{k,l} - \alpha_l \rho_l \varepsilon_l) + \sum_{l=1}^{N} K_{g\,l} (C_{g\,l} k_g - C_{l\,g} k_l) - \sum_{g=1}^{N} K_{g\,l} (\vec{u}_g - \vec{u}_l) \frac{\mu_{t,g}}{\alpha_g \sigma_g} \nabla \alpha_g + \sum_{g=1}^{N} K_{g\,l} (\vec{u}_g - \vec{u}_l) \frac{\mu_{t,l}}{\alpha_l \sigma_l} \nabla \alpha_l \tag{15}$$

$$\frac{\partial}{\partial t}(\rho_l \alpha_l \varepsilon_l) + \nabla \cdot (\rho_l \alpha_l \vec{u}_l \varepsilon_l) = \nabla \cdot \left(\alpha_l \frac{\mu_{t,l}}{\sigma_\varepsilon} \nabla \varepsilon_l \right) + \frac{\varepsilon_l}{k_l} \left[C_{1,\varepsilon} \alpha_l G_{k,l} - C_{2,\varepsilon} \alpha_l \rho_l \varepsilon_l + C_{3,\varepsilon} \left(\sum_{l=1}^{N} K_{g\,l} (C_{g\,l} k_g - C_{l\,g} k_l) - \sum_{g=1}^{N} K_{g\,l} (\vec{u}_g - \vec{u}_l) \frac{\mu_{t,g}}{\alpha_g \sigma_g} \nabla \alpha_g + \sum_{g=1}^{N} K_{g\,l} (\vec{u}_g - \vec{u}_l) \frac{\mu_{t,l}}{\alpha_l \sigma_l} \nabla \alpha_l \right) \right] \tag{16}$$

Term C_{gl} = 2 and C_{lg} are given as:

$$C_{lg} = 2\left(\frac{\eta_r}{1+\eta_r} \right) \tag{17}$$

The turbulent viscosity for each phase *l* is given as follows:

$$\mu_{t,l} = \rho_l C_\mu \frac{k_l^2}{\varepsilon_l} \tag{18}$$

The model constants are similar to those of mixture *k*-ε models.

2.3 Bubble column dimensions and modelling strategy

A cylindrical bubble column was considered with a diameter of 0.19 m, filled with tap water to a height of 0.96 m; a perforated plate sparger was placed at the bottom of the column. The gas superficial velocity was 0.12 m/s. The geometry of the bubble column studied here was similar to the one that has been studied experimentally by Degaleesan [24] and, which has been simulated numerically by Sanyal *et al*. [16] and Chen *et al*. [12].

Usually, fine bubbles introduced by sparger will coalesce immediately when they come in contact with the neighbouring bubbles. The upward movement of the bubble induces the turbulent flow due to upward and downward movement of the liquid phase as the bubble rises. The turbulent flow would then induce the bubble breakage and coalescence, which would attain equilibrium when a certain size of bubble has been obtained. It has to be noted that the gas sparging rate need to be controlled to ensure a better gas dispersion in a bubble column. At lower gas flow rate, the bubble column operates under a homogeneous bubbly flow regime, if the gas flow rate increased even further the flow regime may become turbulent bubbly flow or slug and annular flow for even higher gas flow rate. The flow regime transition in the bubble column cannot be generalised by looking at its relationship with the gas flow rate alone because they are dependent upon many other parameters such as the column geometry, material properties and operating conditions. Further details regarding the flow regime transition in a bubble column may be understood better by referring to a recent review by Shaikh and Al-Dahhan [23].

The Eulerian two-fluid model was employed throughout this study with constant bubble sizes of 3.6 mm, 4.4 mm and 7 mm. The transient solvers with second order implicit time advancement and the third-order (QUICK) spatial interpolation schemes were also applied. The interphase drag coefficient was estimated using the Schiller-Naumann drag model and virtual mass was also included. The top liquid surface was allowed to expand freely as a result of aeration by applying a free surface boundary.

Two grid sizes were evaluated in this study, which is labelled as coarse (Figure 1A) and fine (Figure 1B) generated by

pre-processor software, GAMBIT 2.2. The coarse grid contains 6150 cells and the fine one contains 43460 cells. Both grids were made of a high quality pure hexahedral mesh to minimise the turbulent diffusion during the simulation. Grid refinement was carried out in FLUENT after a steady aeration level was reached based on the aerated water level in the column. The grid refinement was applied in the cells where the water volume fraction is greater than 0.04. Such a method is good for grid economy, because only the section containing liquid will be refined, thus making the excess (headspace) volume just represent a mere 2% of the total cells count. The excess volume in the headspace is necessary because at the initial stages of the simulation, there are some major fluctuations of the liquid surface; without this excess volume, some part of the liquid would flow out from the domain and hence may cause error to the final result. This incidence is shown in Figure 2 which was simulated using a grid of only 1.4 m height. In the third frame, the aerated level exceeds the upper bound of the flow domain, which is unacceptable. In light with this issue, the final grid height was extended up to 1.5 m, to provide a more satisfactory simulation. The evidence of a turbulent bubbly flow is also depicted in Figure 2 as the flow becomes unstable and the bubbles cluster into swarms, hence regions of relatively high and low gas fractions can be distinguished. The motion of swarms through the column is highly irregular and the swarms only exist for a short period of time [18]. The swarms dominate the hydrodynamic behavior of a bubble column by increasing the degree of (back) mixing or dispersion of the liquid phase leading to larger-scale circulation patterns. The long-time-averaged liquid flow field shows a large overall liquid circulation pattern with the liquid phase flows upward in the centre of the column and downward in the wall region [18].

The coarse grid employed in this work may not be capable of resolving correctly the turbulence related quantities (k and ε), but it is assumed to have a limited effect in this study, since the bubble size distribution model is not included; instead bubble is assumed to be monodispersed in this study. The turbulence related quantities must be resolved for better prediction of bubble size when a bubble size distribution model is employed as the turbulent dissipation rates have a great influence on bubble coalescence and break-up. All result presented in this chapter are taken at $z = 0.53$ and are time-averages of up to 1000 time step after a steady aerated liquid level is attained. During the initial simulation prior to achieving the pseudo-steady aerated liquid level a much larger time step of 0.01 s was employed. The time step was reduced to 0.005 s for the final simulation and were averaged for the real time of 5 seconds.

Water with a volume fraction of 1.0 is patched to $0 \leq z \geq 0.96$ (initial liquid height) before running the simulation, whereas water volume fraction of 0 is patched to the headspace ($0.96 \leq z \leq 1.5$). Air is sparged at the bottom of the column using a velocity inlet boundary (gas inlet velocity equal to superficial gas velocity) as soon as the simulation started (time = 0 s).

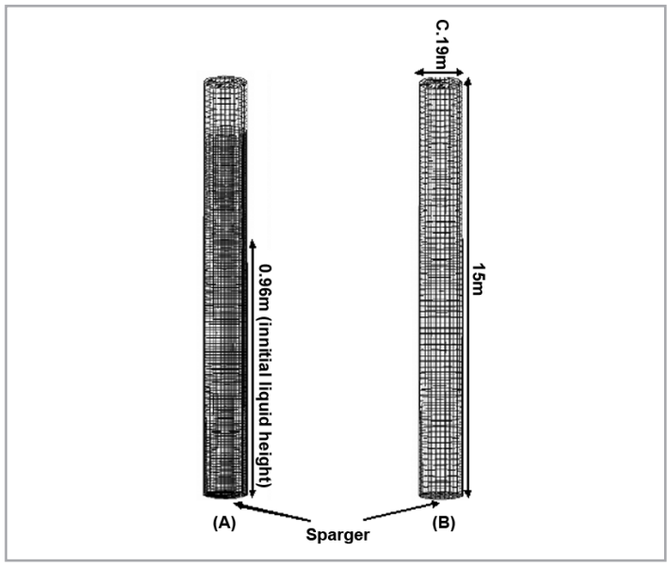

Figure 1: Surface mesh of the bubble column , A) Coarse mesh, B) Fine mesh

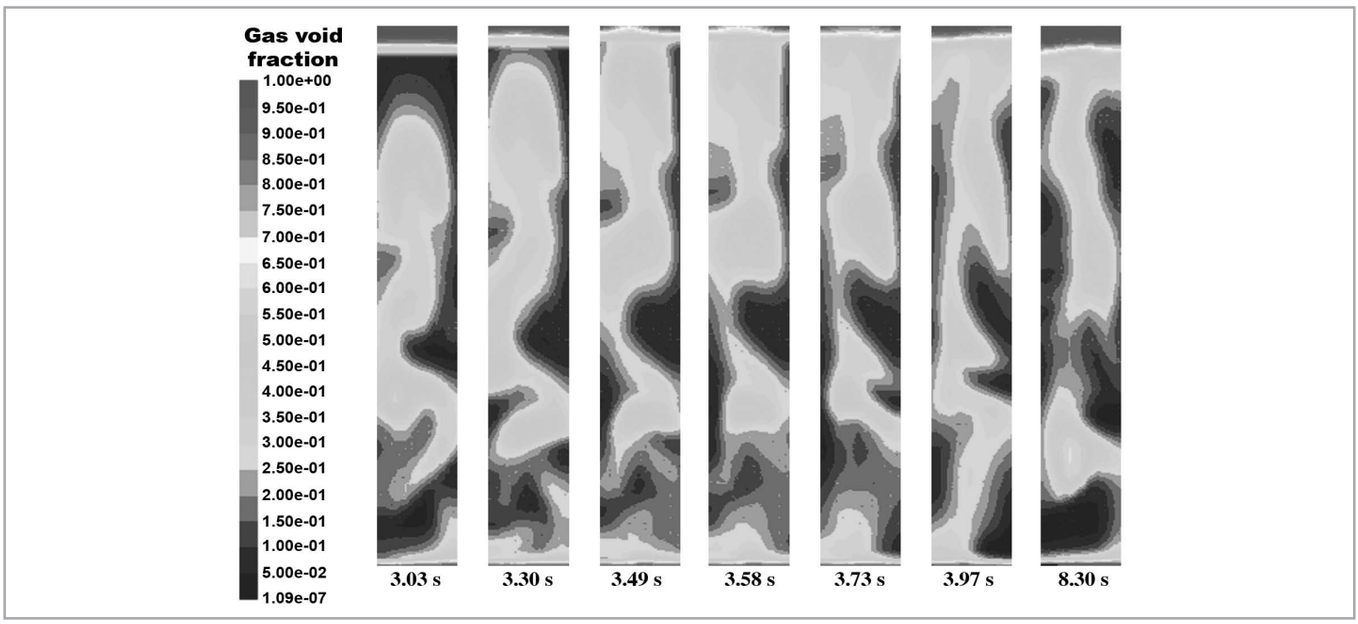

Figure 2: Illustration of liquid overflowing from the flow domain (t = 3.49~3.58 s) in the initial stage of the simulation for the case with grid height of 1.4 m. The image is coloured by gas volume fraction and so the red upper layer represents the headspace

3.0 RESULTS AND DISCUSSIONS

3.1 Effect of the bubble size

Correlations to estimate the mean bubble size are often related to liquid surface tension (σ), liquid density (ρ_l), liquid viscosity (μ_l) and gas superficial velocity (v_{sg}). Some correlations include the gas density (ρ_g) and gravity (g) as well, such as the one proposed by Wilkinson [25]:

$$d_b = 3g^{-0.44}\,\sigma^{0.34}\,\mu_l^{0.22}\,\rho_l^{-0.45}\,\rho_g^{-0.11}\,v_{sg}^{-0.02} \quad (19)$$

Another correlation of bubble size proposed by Pohorecki *et al*. [26] is:

$$d_b = 0.289\,\sigma^{0.442}\,\mu_l^{-0.048}\,\rho_l^{-0.552}\,v_{sg}^{-0.124} \quad (20)$$

Both correlations give a mean bubble size less than 5 mm *i.e.* 4.4 mm for Wilkinson and 3.6 mm for Pohorecki. These values are in good agreement with Deen *et al*.'s [10] experiments, which observed a 4 mm mean bubble diameter in his study on a rectangular bubble column of air-water system.

Comparisons of the CFD prediction for the three different bubble sizes are shown in Figures 3 and 4, alongside the experimental data of Degaleesan [24]. There is no noteworthy difference between the liquid axial velocity and gas hold-up calculated using the bubble size of either 4.4 mm or 3.6 mm (Figure 5.4), maybe because the difference of the bubble size is just a mere 0.8 mm and thus the effect is insignificant. Meanwhile, both the gas hold-up and liquid axial velocity were underpredicted when the 7 mm bubble diameter was applied. This underprediction of the gas hold-up is due to the fact that bigger bubbles tend to rise faster than smaller ones and thus the gas volume fraction in the liquid is reduced. The liquid velocity is affected by the bubble size: bigger bubbles might increase the axial velocity due to their larger bubble rise velocity but at the same time the downward recirculation also becomes larger. In fact, the momentum from the liquid recirculation is bigger than the one induced by bubble rise velocity, and therefore a bigger bubble size leads to a lower axial liquid velocity.

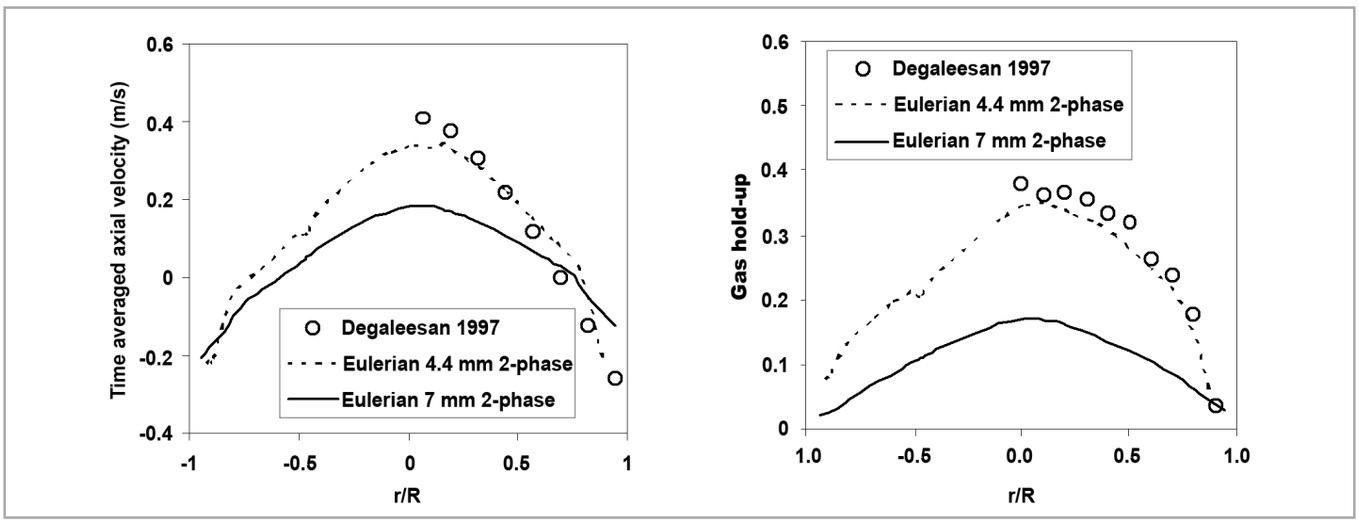

Figure 3: Effect of bubble size on gas hold-up and axial liquid velocity, modelling were carried out using the fine grid

3.2 Assessment of the modelling grid

The initial grid was quite coarse (approx 2 x 2 x 1.5 cm) and contained only 6150 computational cells as shown in Figure 1A. Initial iterations were carried out on the coarse grid until a pseudo-steady aerated liquid height was reached. Then a grid adaptation was applied in the region where the water volume fraction was greater than 0.4 (up to the aerated liquid height). As a result a relatively fine grid containing 43 460 cells (see Figure 1B) was created. For grid assessment purpose, the simulation was then carried out using both grids with the mixture k-ε model for turbulence and the two phase flow was modelled via the Eulerian-Eularian model. The mixture k-ε model itself uses exactly similar equation to the standard k-ε formulation, except that the physical and thermodynamic properties of the mixture are applied.

The effect of grid size on two-phase flow in a bubble column is presented in Figure 4. It was found that the finer grid gave a slightly higher peak of the gas hold - up and liquid axial velocity, as shown in Figure 4, which is closer to Degaleesan's experimental data. Finer grids also help to resolve correctly the gas hold-up and liquid axial velocity very close to the wall, which is not shown in a coarser grid. Therefore, the finer grid will be employed for the rest of the study in this case as it gave much closer agreement with Degaleesan's experimental data. The use of a finer grid, however, poses a significant increase in computational effort with nearly ten times slower iterations than the coarser one. It should be noted that effect of the grid refinement is not very obvious in this study due to several reasons. Firstly, the grid employed in this work are made of pure hexahedral aligned to the mean flow direction hence minimising the turbulent diffusion thus resulting in better prediction. Secondly, the close agreement between the result obtained from both fine and coarse grid actually confirming a grid independent solution has been achieved.

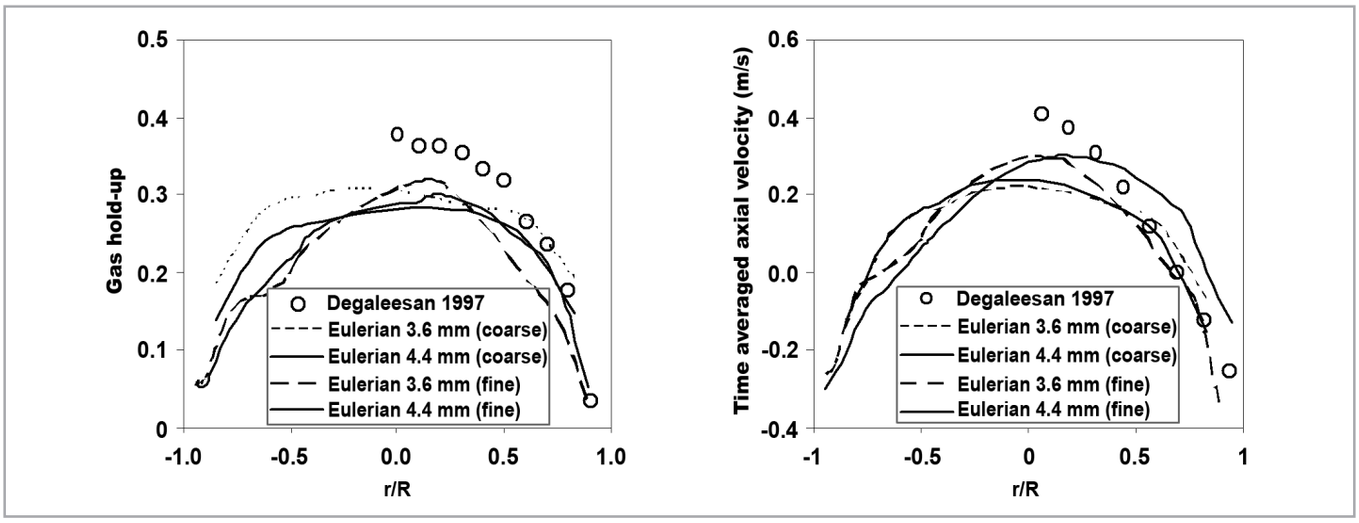

Figure 4: Prediction of gas hold-up and axial liquid velocity by mixture turbulence model for different grid resolution

3.3 Assessment of the turbulence models

There are three turbulence model available for multiphase modelling in FLUENT namely, mixture *k*-ε, dispersed *k*-ε and two-phase *k*-ε. The mixture model is said to be suitable for a system with a fluid density ratio close to 1, *e.g.* hexanol-water system. The dispersed model is applicable when there is clearly one primary continuous phase and the remainder is a dilute secondary phase. The two-phase turbulence model is said to be an appropriate choice when the turbulence transfer among the phases plays a dominant role. However, it should be noted that the two-phase model is two times more computational intensive than either the dispersed or the mixture models, since the turbulence model must be solved for both phases for each iteration. Since there are no recommendations or comparisons available elsewhere, the predicting capability of all three turbulence models on the two-phase flow in a bubble column have been evaluated. All simulations were performed using the refined grid and the two-phase flow was modelled via the Eulerian-Eulerian two-fluid model.

Predictions of the different turbulence model on the axial velocity and the gas hold-up are shown in Figure 5. The results clearly show that two-phase turbulence model gives much closer agreement with Degaleesan's [24] experiments. This is to be expected as the superficial gas velocity is quite high at 0.12 m/s, which corresponds to 30% gas hold-up in the bubble column. Poor prediction of multiphase flows by mixture model is explained by the fact that it is more suitable for a multiphase system with nearly similar densities. Meanwhile, the dispersed model is more suitable for a dilute secondary phase, which is not the case in this simulation.

It is not always clear from the literature to why some previous researchers have been able get a good prediction of the gas hold-up and liquid velocity profile using the dispersed *k*-ε model at high void fraction. According to Chen *et al.* [12], the input bubble size might be tweaked to get a better fit to the experimental data, which they demonstrated in their study. However, this is not really an acceptable solution because a good model should be able to predict the two-phase flow field without any tuning and hence becoming fully predictive.

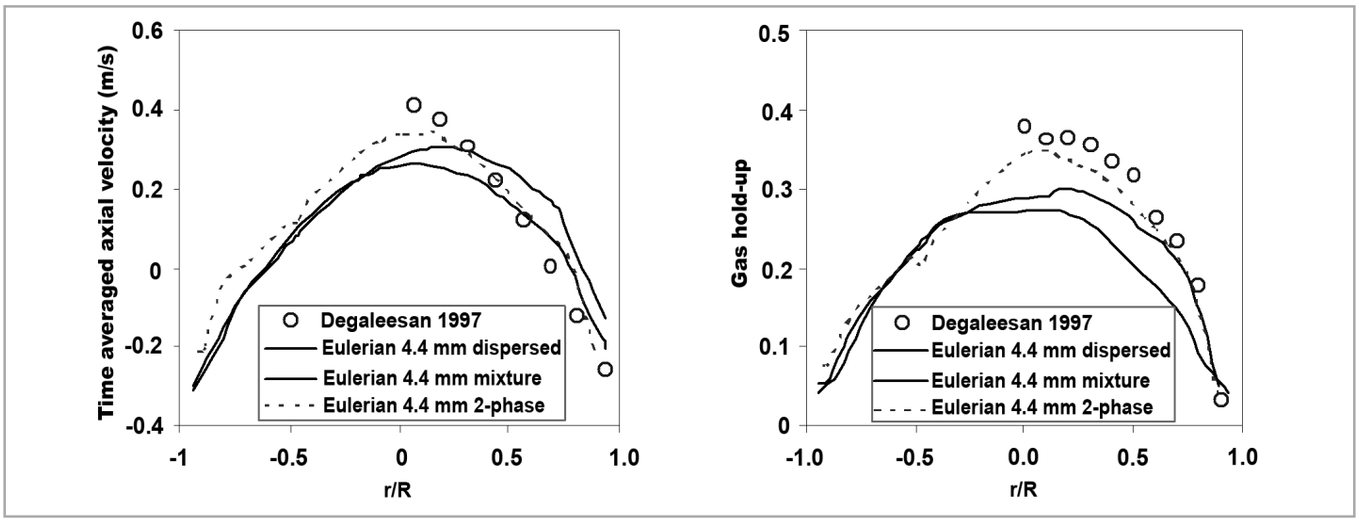

Figure 5: Prediction of liquid axial velocity and gas hold-up by different turbulent model, modelling were carried out using the fine grid

6.0 CONCLUSIONS

Modelling of gas-liquid flow in a bubble column has been successfully carried out using the Eulerian two-fluid approach. The results suggest that the prediction accuracy can be significantly affected by the bubble size, the grid resolution and selection of the turbulence model. Findings from this modelling exercise may be useful for design and troubleshooting of bubble columns, in particular when dealing with selection of the turbulence model. Bubble size has a great influence on the gas-liquid flow in bubble columns because they affect directly the interphase forces between gas and liquid. Findings from this work suggest that Wilkinson's [25] correlation is sufficient to yield a reasonably correct bubble size in a bubble column, reflected by the correct prediction on gas-liquid hydrodynamics. It also noted that the assumption of a constant bubble size is sufficient to yield a good prediction of the gas hold-up and liquid velocity in a bubble column.

It is necessary to have a sufficiently fine grid for gas-liquid simulation, as the coarser grid may not be small enough to resolve the multiphase flow pattern. In the case where the experimental data are available, grid refinement need to be applied until a reasonable agreement is obtained. If the experimental data are not available, a grid independence analysis might be necessary.

Selection of an appropriate turbulence model for gas-liquid modelling is highly dependent on the void fraction of the dispersed phase. When the void fraction of the dispersed phase is high (up to 30% gas hold-up), such as in the case studied in this work, the two-phase turbulence model seems to be more appropriate. ■

NOTATIONS

C_D drag coefficient
C_L lift coefficient
C_m virtual mass coefficient
$C_{\varepsilon 1}$ constant for eqs.(8, 14, and 16)
$C_{\varepsilon 2}$ constant for eqs.(8, 14, and 16)
d_b bubble size
$\vec{F}_g$ interaction force mainly due to drag
$\vec{F}_{lift}$ lift force
$\vec{F}_{vm}$ virtual mass force
g gravity acceleration
G_k turbulent production term
k turbulent kinetic energy
K_{gl} interphase momentum exchange coefficient
P pressure
v_{sg} superficial gas velocity
Re_b bubble Reynolds number
t time
u, v velocity components
u_{slip} slip velocity
u_t turbulent viscosity

Greek

α void fraction
ε turbulent dissipation rate
ρ density
σ_ε constant for eqs.(8, 14, and 16)
σ_k constant for eqs.(7, 13, and 15)
$\prod_{k,l}$ characteristic turbulent kinetic energy for secondary phase
$\prod_{\varepsilon,l}$ characteristic turbulent dissipation rate for secondary phase
$\bar{\bar{\tau}}_l$ liquid phase stress-strain tensor
μ_l liquid viscosity

Subscripts

b bubble
g gas
l liquid
m mixture
i mixture entity of i phase

REFERENCES

[1] F. Barriga-Ordonez, F. Nava-Alonso, and A. Uribe-Salas, "Cyanide oxidation by ozone in a steady-state flow bubble column", *Minerals Engineering*, Vol. 19, No. 2, pp. 117-122, February 2006.

[2] S.M. Mousavi, A. Jafari, S. Yaghmaei, M. Vossoughi, and I. Turunen, "Experiments and CFD simulation of ferrous biooxidation in a bubble column bioreactor", *Computers & Chemical Engineering*, Vol. 32, No. 8, pp. 1681-1688, August 2008.

[3] S.-W. Kang, S.-W. Kim, and J.-S. Lee, "Production of cellulase and xylanase in a bubble column using immobilized Aspergillus Niger KKS", *Journal Applied Biochemistry and Biotechnology*, Vol. 53, No. 2, pp. 101-106, May 1995.

[4] A.S. Chaudhari, M.R. Rampure, V.V. Ranade, R. Jaganathan, and R.V. Chaudhari, "Modeling of bubble column slurry reactor for reductive alkylation of p-phenylenediamine", *Chemical Engineering Science*, Vol. 62, No. 24, pp. 7290-7304, December 2007.

[5] A.H. Konsowa, "Decolorization of wastewater containing direct dye by ozonation in a batch bubble column reactor", *Desalination*, Vol. 158, No. 1-3, pp. 233-240, August 2003.

[6] N. Rados, M.H. Al-Dahhan, and M.P. Dudukovic, "Modeling of the Fischer-Tropsch synthesis in slurry bubble column reactors", *Catalysis Today*, Vol. 79-80, pp. 211-218, April 2003.

[7] H. Ishibashi, M. Onozaki, M. Kobayashi, J. -i. Hayashi, H. Itoh, and T. Chiba, "Gas hold-up in slurry bubble column reactors of a 150 t/d coal liquefaction pilot plant process", Fuel, Vol. 80, No. 5, pp. 655-664, April 2001.

[8] Y.T. Shah, B.G. Kelkar, S.P. Godbole, and W.-D. Deckwer, "Design parameter estimations for bubble column reactors", *The American Institute of Chemical Engineers Journal*, Vol. 28, No. 3, pp. 353-379, 1982.

[9] K. Ekambara, M.T. Dhotre, and J.B. Joshi, "CFD simulations of bubble column reactors: 1D, 2D and 3D approach", *Chemical Engineering Science*, Vol. 60, No. 23, pp. 6733-6746, December 2005.

[10] N.G. Deen, T. Solberg, and B.H. Hjertager, "Large eddy simulation of the gas-liquid flow in a square cross-sectioned bubble column", *Chemical Engineering Science*, Vol. 56, No. 21-22, pp. 6341-6349, November 2001.

[11] R. Krishna, M.I. Urseanu, J.M. Van Baten, and J. Ellenberger, "Influence of scale on the hydrodynamics of bubble columns operating in the churn-turbulent regime: Experiments vs. Eulerian simulations", *Chemical Engineering Science*, Vol. 54, No. 21, pp. 4903-4911, November 1999.

[12] P. Chen, J. Sanyal, and M.P. Duduković, "Numerical simulation of bubble columns flows: Effect of different breakup and coalescence closures", *Chemical Engineering Science*, Vol. 60, No. 4, pp. 1085-1101, February 2005.

[13] T. Wang, J. Wang, and Y. Jin, "Theoretical prediction of flow regime transition in bubble columns by the population balance model", *Chemical Engineering Science*, Vol. 60, No. 22, pp. 6199-6209. November 2005.

[14] R. Bannari, F. Kerdouss, B. Selma, A. Bannari, and P. Proulx, "Three-dimensional mathematical modeling of dispersed two-phase flow using class method of population balance in bubble columns", *Computers & Chemical Engineering*, Vol. 32, No. 12, pp. 3224-3237, December 2008.

[15] M.T. Dhotre, B.L. Smith, B. and Niceno, CFD simulation of bubbly flows: Random dispersion model, *Chemical Engineering Science*, Vol. 62, No. 24, pp. 7140 – 7150, December 2007.

[16] J. Sanyal, S. Vásquez, S. Roy and M.P. Dudukovic, "Numerical simulation of gas-liquid dynamics in cylindrical bubble column reactors", *Chemical Engineering Science*, Vol. 54, No. 21, pp. 5071-5083, November 1999.

[17] M.T. Dhotre, and J.B. Joshi, "Two-dimensional CFD model for the prediction of flow pattern, pressure drop and heat transfer coefficient in bubble column reactors", *Chemical Engineering Research and Design*, Vol. 82, No. 6, pp. 689-707, June 2004.

[18] J. S. Groen, "Scales and structures in bubbly flows", PhD Thesis, Delft University of Technology, The Netherlands, 2004.

[19] L. Schiller, and Z. Naumann, "A drag coefficient correlation", Zeitschrift Verein Deutscher Ingenieure, 77, pp. 318-320, 1935.

[20] FLUENT 6.3, User Guide, 2006.

[21] S.E. Elgobashi, and T.W. Abou-Arab, "A Two-Equation Turbulence Model for Two-Phase Flows", *Physic of Fluids*, Vol. 26, No. 4, pp. 931-938, 1983.

[22] R. Mudde, and O. Simonin, "Two- and three-dimensional simulations of a bubble plume using a two-fluid model", *Chemical Engineering Science*, Vol. 54, No. 21, 5061–5069, November 1999.

[23] A. Shaikh, and M. Al-Dahhan, "A Review on Flow Regime Transition in Bubble Columns", *International Journal of Chemical Reactor Engineering*: Vol. 5: R1, 2007.

[24] S. Degaleesan, "Fluid dynamic measurements and modeling of liquid mixing in bubble columns", *D.Sc. Thesis*, St. Louis, Missouri, USA: Washington University, 1997.

[25] P.M. Wilkinson, "Physical Aspects and Scale-up of High Pressure Bubble Columns", *D.Sc. Thesis*, University of Groningen, The Netherlands, 1991.

[26] R. Pohorecki, W. Moniuk, P. Bielski, and P. Sobieszuk, "Diameter of bubbles in bubble column reactors operating with organic liquids", *Chemical Engineering Research and Design*, Vol. 83, No. 7, pp. 827-832, July 2005.

PROFILE

DR JOLIUS GIMBUN

Dr J. Gimbun is a lecturer at Faculty of Chemical and Natural Resources Engineering of Universiti Malaysia Pahang. He has a B.Eng. (Chem. Eng.) and M.Sc. Research (Env. Eng.) from UPM, as well as a Ph.D. (Chem. Eng.) from Loughborough University, UK. Dr Gimbun specialise in computer simulation, mainly on CFD and population balance modelling. He has over 6 years experience in CFD, where he has been involved in a wide range of activities varying from algorithm development to complex flow simulation. He had performed major CFD simulations on aerocyclones, mixing tanks, bubble columns, spray dryings, spray freeze dryings, gas-liquid stirred tanks, ceramic filters and monolithic reactors. Dr Gimbun also serves as a regular referee for many international journals such as *AIChE J., Chem. Eng. Sci., Chem. Eng. J., Powder Technol., Separation and Purif. Technol., Computer and Chem. Eng., and Part. and Part. Sys. Charac.*, among others. He is currently a member of IChemE UK, FMPSG UK, IEM, IMM and also a registered engineer with BEM. His official website is http://chem.ump.edu.my/name.cfm?